Industrial Engineering Journal
ISSN: 0970-2555
Volume : 54, Issue 8, No.1, August : 2025

LIFE CYCLE COST ANALYSIS OF NATM USING ANN

Mayur Jadhav ME Student, Department of Civil Engineering, Pillai HOC College of Engineering and Technology, Rasayani University of Mumbai.
Dr. Madhulika Sinha Department of Civil Engineering, Pillai HOC College of Engineering and Technology, Rasayani University of Mumbai.

ABSTRACT
The New Austrian Tunneling Method (NATM) is a widely adopted tunneling technique known for its flexibility and cost-effectiveness in various geotechnical conditions. However, the complexity of NATM construction processes and the variability of geological factors make accurate cost estimation challenging. This study focuses on conducting a comprehensive Life Cycle Cost Analysis (LCCA) of NATM projects by integrating Artificial Neural Networks (ANN) as a predictive modeling tool. LCCA evaluates the total cost of a project over its entire lifespan, including initial construction, maintenance, and operation, providing a holistic economic assessment. ANN, with its ability to model complex nonlinear relationships and learn from historical data, is utilized to predict the life cycle costs more accurately than traditional methods. The research involves collecting extensive data from completed NATM tunneling projects, including geological parameters, construction variables, and cost elements. This data is used to train and validate the ANN model, enabling it to predict cost outcomes under varying conditions effectively. The results demonstrate that ANN can significantly enhance the precision of cost forecasting, facilitating better decision-making and budget planning. Moreover, the integration of LCCA with ANN supports stakeholders in optimizing resource allocation and mitigating financial risks throughout the tunnel's operational life. This study contributes to the field by offering an innovative approach that combines geotechnical engineering with advanced machine learning techniques to improve economic evaluations of complex tunneling projects, promoting sustainable infrastructure development.

1. INTRODUCTION
The incorporation of Artificial Neural Networks (ANN) into the Life Cycle Cost (LCC) analysis of the New Austrian Tunnelling Method (NATM), a popular method in tunnel building because of its adaptability and flexibility in a variety of geological settings, is examined in this paper. LCC analysis is crucial to NATM's performance since it depends on careful planning and efficient cost management. From design and construction to operation and maintenance, LCC analysis evaluates every expense related to a project across its entire lifecycle [1]. By taking into consideration initial investments, future repairs, and operating expenditures, it makes it possible to identify long-term cost-efficient alternatives. Such thorough analysis aids stakeholders in selecting the most cost-effective options for tunnel construction without sacrificing project specifications or safety [2]. However, conventional LCC analysis techniques often fail to adequately capture the intricacy and unpredictability's present in tunnelling projects. In order to get around this, the research uses artificial neural networks, a potent computing technique that improves decision-making and prediction accuracy. Large amounts of historical data may be processed by ANNs, which can also identify intricate patterns and predict future expenses based on a variety of influencing factors, such as geological conditions, building methods, and material selections. A more responsive and realistic cost model is made possible by their capacity for learning and adaptation [3]. The goal of this project is to provide an intelligent, data-driven framework for cost prediction and optimization by using ANN in LCC analysis for NATM [4]. In addition to increasing accuracy, this method gives engineers and project managers the ability to reduce financial risks, maximize resources, and guarantee that safety

regulations are followed. Modernizing the financial planning and administration of tunnelling infrastructure has advanced significantly thanks to the combination of ANN and conventional cost analysis.

2. LITERATURE REVIEW

Recent innovations in Life Cycle Cost Analysis (LCCA) in the building and infrastructure sectors show a rising focus on merging conventional cost estimating methodologies with modern computer technology. For example, emphasise the significance of Environmental Product Declarations (EPDs) as the basis of sustainable building evaluation, with Life Cycle evaluation (LCA) playing a critical role[5]. Their worldwide research identified 27 significant hurdles to applying LCA for EPDs, which were divided into seven categories. These included data quality, methodological restrictions, and technology limits. The study emphasises the critical need for high-quality data and improved methods to improve LCA dependability, which directly affects the credibility of EPDs. Similarly, Artificial Neural Networks (ANNs) were shown to be useful in developing a cost model for road tunnels [6]. By analysing cost components over a 75-year period, their model, which was used to the Enatic Odours Motorway in Greece, provided infrastructure managers with a precise tool for financial forecasting and planning. ANN-based models are increasingly being employed in industries where cost accuracy and flexibility to changing factors are critical. Dynamic LCCA was applied to historic site conservation using the MONUREV V2 program, demonstrating how scenario modelling may inform balanced cultural and economic decisions [7]. Compared ANN and regression models for LCC prediction at the early design phase, showing ANN's better accuracy when early-stage data is limited [8]. Aleksandra Murkowski et al. (2022) supported this trend by examining the literature on combining Environmental Life Cycle Costing (ELCC) with Machine Learning (ML), indicating that ML improves the accuracy and sustainability of project choices. Meanwhile, a Revit plug-in connected BIM with LCCA, allowing designers to conduct real-time scenario analysis that included operational and maintenance considerations, enabling educated and sustainable building design decisions [9].

The scope of ANN applications in LCCA includes industrial systems and public infrastructure. focused on pumping systems, comparing healthy and malfunctioning states using a hybrid SVM-HMM model [10]. Their AI-based technique allowed for early defect identification and considerable energy cost reductions. LCA and LCCA are underutilised in geotechnical engineering, and better frameworks are needed to help engineers reduce life cycle costs [11]. analysed LCCA in transport infrastructure, proposing for the inclusion of social and user costs, notwithstanding measurement difficulties [12]. These results are consistent with the work of others who examined green construction projects in Indonesia using LCCA and found long-term environmental and economic advantages despite greater upfront expenses. Deep Neural Networks (DNNs) were presented as a replacement for simulation-based LCCA in asset management systems, which considerably reduced computing time and improved decision-making for massive infrastructure datasets [13]. Several studies provide useful insights about tunneling-specific circumstances [14]. proposed an ANN and Cost Significant Item (CSI) architecture to ease LCCA in construction, resulting in high estimate accuracy in case studies [15]. Machine learning was used with geophones in tunnelling projects to automate paperwork and improve predictive maintenance [16]. suggested a tunnel data format for NATM that uses BIM-compatible IFC extensions to assist digitise tunnel design components [17]. solved the difficulty of handling huge datasets from NATM tunnel monitoring using a big-data-enabled data service system, resulting in better planning and resource utilisation. created a planning-stage approach employing case-based reasoning to predict environmental loads in tunnel construction, which outperformed established techniques in terms of accuracy [18]. These

studies highlight the growing need for digital tools to handle data complexity and enhance decision support in NATM-based tunnelling.

3. RESEARCH METHOD

Life Cycle Cost Analysis (LCCA) has become an essential tool for evaluating the long-term economic performance of infrastructure projects. When applied to tunneling projects utilizing the New Austrian Tunneling Method (NATM), LCCA becomes even more crucial due to the method's inherent complexities, including variable geological conditions, diverse construction techniques, and long operational lifespans[19]. Traditionally, estimating the costs associated with such projects has been challenging. However, the integration of Artificial Neural Networks (ANN) into LCCA presents a modern, data-driven solution that significantly improves predictive accuracy and decision-making[20]. ANN models, capable of learning from large sets of historical data, offer the ability to recognize hidden patterns in cost-related factors—ranging from excavation and material usage to labor and environmental conditions. By training ANN with real-world NATM project data, we can anticipate not only initial construction costs but also long-term expenses such as maintenance, energy consumption, and rehabilitation efforts[21]. Furthermore, the synergy between ANN and tools like ANSYS simulations—used for finite element analysis allows the model to incorporate both empirical data and structural behavior insights, enabling a comprehensive and realistic approach to cost forecasting[22]. This integration facilitates optimized resource allocation, identification of key cost drivers, and enhanced risk mitigation, ultimately contributing to the financial sustainability of NATM tunneling projects.

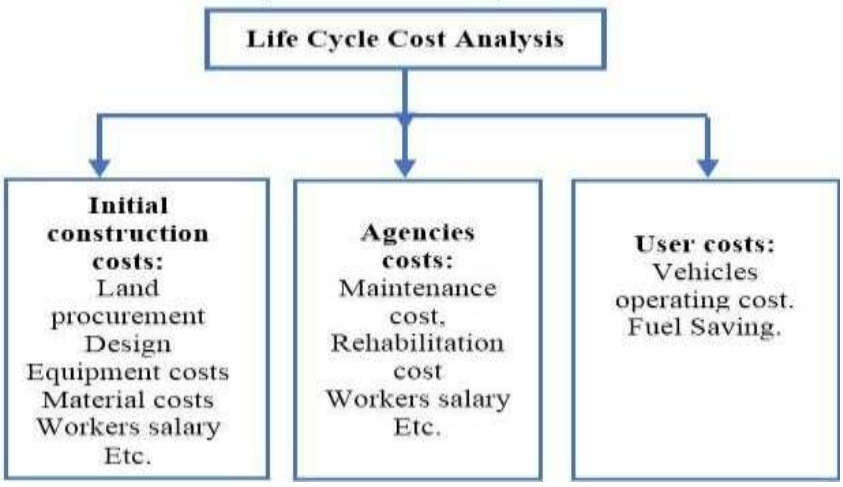

3.1 Methodology and Economic Indicators in LCCA

The methodology for conducting a Life Cycle Cost Analysis in NATM projects using ANN involves several structured steps. Initially, costs related to construction and maintenance are estimated using the Net Present Value (NPV) method, guided by standards such as IRC SP-30 (2009). This approach involves calculating the present value of all costs and benefits across the project's lifecycle, adjusting for time using discount rates[23]. The four primary steps include estimating initial construction costs, ongoing maintenance, road user costs, and conducting a comprehensive life-cycle cost and benefit analysis using ANN. To support economic evaluation, several indicators are employed, including NPV, Cost-Benefit Ratio (B/C), Equivalent Uniform Annual Costs (EUAC), and Internal Rate of Return (IRR). Each has unique applicability based on project scope, decision-making level, and economic context. For instance, in cases with equal benefits across alternatives, NPV is the most effective indicator for comparing differing

cost scenarios. NPV's additive nature simplifies computation by focusing solely on differential costs. The economic analysis framework helps decision-makers determine how capital investments weigh against future expenditures, and which analysis method is most suited for the agency's goals[24]. Through this lens, the LCCA methodology not only quantifies costs but supports strategic planning and investment decisions.

3.2 Data Collection and ANN Model Development

A successful ANN model for LCCA depends heavily on the quality and comprehensiveness of historical data collected from NATM projects. This includes data on construction, operational, maintenance, and rehabilitation costs. Construction data covers excavation, labor, materials, machinery, and unforeseen costs due to geological surprises. Operational costs relate to energy consumption, utilities, and staffing, while maintenance and rehabilitation data focus on regular and major upkeep efforts[25]. Additionally, geological data—such as rock types, stability, and groundwater presence—profoundly affects tunnel behavior and costs. Other crucial data includes material usage, labor costs, and environmental conditions like temperature and seismic activity. These diverse data points are obtained from project reports, cost estimation documents, sensor-based monitoring systems, and real-time construction data. Once data is collected, ANN model development involves identifying input variables (e.g., geological factors, excavation techniques, construction methods) and output variables (e.g., total cost, maintenance cost). The network architecture is built with input, hidden, and output layers. ReLU is typically chosen as the activation function for its efficiency in handling large datasets[26]. The model is trained using backpropagation, where errors between predicted and actual outputs are minimized through iterative weight adjustments. This enables the ANN to effectively model the complex relationships within NATM project cost components.

3.3 Model Validation, Testing, and Practical Application

After developing the ANN model, rigorous validation and testing are essential to ensure its reliability and applicability in real-world NATM projects[27]. The dataset is typically split into training, validation, and test sets. The training set teaches the model to understand cost patterns, while the validation set helps refine parameters and prevent overfitting. The final evaluation is done using the test set to ensure that the model generalizes well to new data[28]. To further improve robustness, k-fold cross-validation is employed, where data is divided into multiple subsets and used in various combinations for training and validation[29]. This enhances the model's generalization capability and reduces the risk of bias from any single data segment. Performance metrics such as Mean Squared Error (MSE) and R-squared (R^2) are used to assess the model's predictive accuracy. A low MSE and high R^2 indicate that the model accurately captures the underlying relationships in the data. Ultimately, a well-trained ANN model enables precise forecasting of NATM project costs throughout their lifecycle, supporting better financial planning, design evaluation, and risk management. This modern approach transforms how tunneling projects are assessed economically, promoting long-term sustainability and operational efficiency in the infrastructure sector[30].

4. RESULT AND DISCUSSION

The provided data presents a comprehensive analysis of the annual maintenance costs, life cycle expenses, and predictive modeling of tunnels with both rigid and flexible pavements over a 30-year horizon. Utilizing artificial neural networks (ANNs), the study models maintenance cost predictions and evaluates their accuracy through performance metrics such as mean squared error (MSE) and correlation coefficients (R-values). The ANN architectures involve single hidden layers processing input data to forecast multi-

dimensional outputs, reflecting the complex relationships in maintenance cost dynamics influenced by inflation and discount rates.

Cost analyses reveal that while rigid pavements incur higher initial expenses, they become more cost-effective than flexible pavements beyond the break-even point around 2030, with a total life cycle cost advantage of approximately 4.24% by 2048. The data also highlights the significance of discounting future costs at a 12% rate, showing that early investment dominates the net present value (NPV). Predictive models demonstrate strong accuracy in long-term forecasting, particularly for rigid pavements, despite some underestimation of early volatility. Additionally, training curves and validation plots emphasize the balance between fitting accuracy and avoiding overfitting through early stopping. Overall, the integration of machine learning with economic analysis offers valuable insights for infrastructure planning, indicating that rigid pavement tunnels may provide better economic returns over time despite higher upfront costs, supported by robust predictive modeling to guide maintenance scheduling and budgeting.

4.1 Annual maintenance for Tunnel + Rigid Tunnel

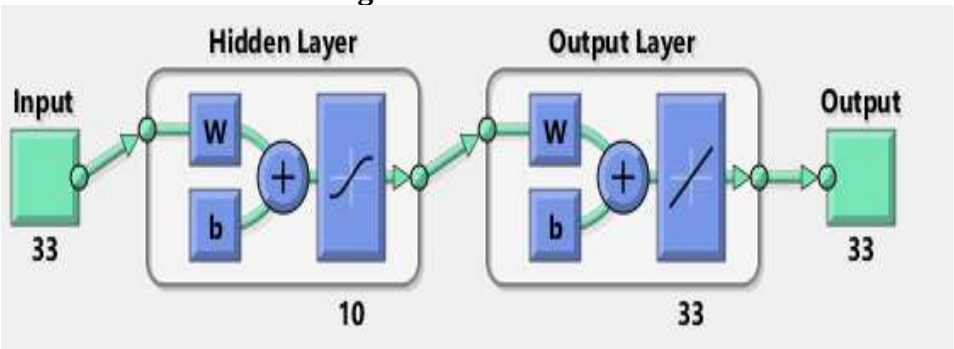

Figure no.1: Annual maintenance for Tunnel + Rigid Tunnel

The provided image shows a simple feedforward neural network architecture with one hidden layer. The input layer has one node with a value of 33. This input is fed into the hidden layer, which consists of 10 neurons. Each neuron in the hidden layer applies a weighted sum (represented by "W") and bias ("b") followed by an activation function (indicated by the curve symbol). The processed outputs from the hidden layer then flow into the output layer, which has 33 neurons. Similar operations occur in the output layer—weighting, bias addition, and activation. The final output layer produces a 33-dimensional output vector. This network is likely used for regression or classification tasks where the input and output sizes are explicitly defined.

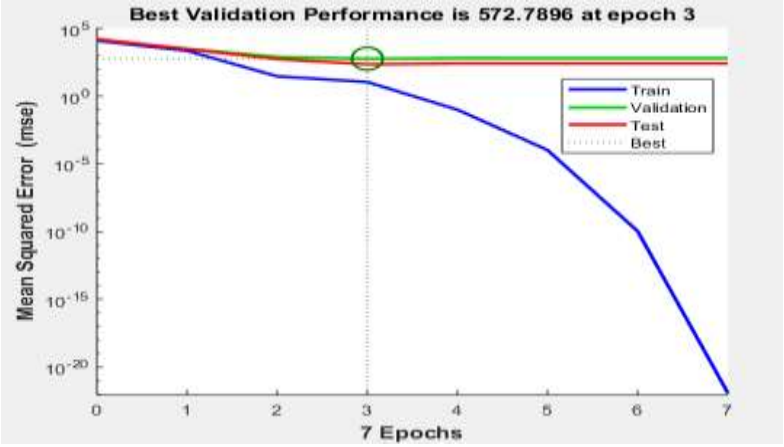

Figure no.2: Best Validation

Industrial Engineering Journal
ISSN: 0970-2555
Volume : 54, Issue 8, No.1, August : 2025

The image shows a plot of Mean Squared Error (MSE) against epochs for training, validation, and testing phases of a model. The plot is logarithmic on the y-axis. It highlights the best validation performance at epoch 3, with a value of 572.7896. At this epoch, the validation error (green line) reaches its minimum, indicating optimal model performance without overfitting. The training error (blue line) continuously decreases, showing the model's learning progress, while the test error (red line) remains steady, closely matching validation error. A green circle marks the best validation point, and a vertical dashed line emphasizes epoch 3. This graph helps to decide the stopping point during training to avoid overfitting while ensuring generalization. The best epoch is identified by the lowest validation MSE, supporting model selection in machine learning.

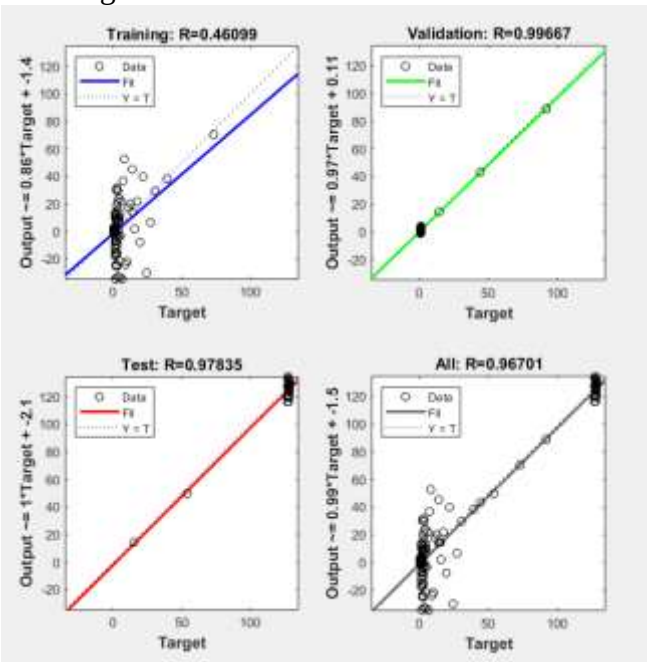

Figure no.3: Best Training, Validation and Test

The image presents regression analysis results for a predictive model evaluated on training, validation, test, and combined datasets. The correlation coefficients (R-values) indicate the model's performance: Training (R = 0.46099) shows moderate correlation, while Validation (R = 0.99667) and Test (R = 0.97835) show very high correlation, implying strong predictive accuracy on unseen data. The overall dataset has an R-value of 0.96701, confirming good model generalization. The plots depict fitted lines closely following the ideal line (Y = T) for validation and test sets, whereas training data shows more scatter, suggesting some underfitting or noise.

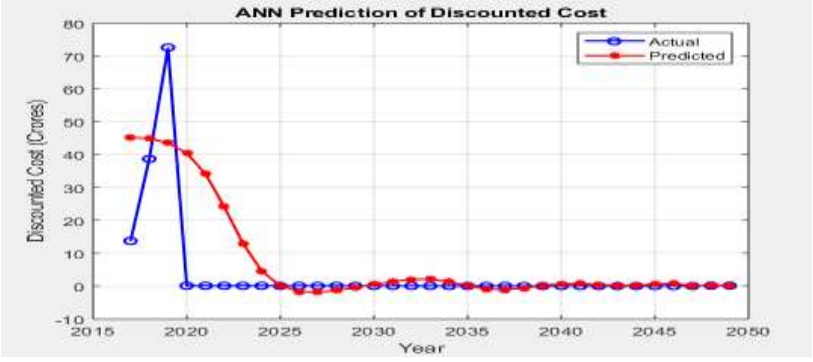

Industrial Engineering Journal
ISSN: 0970-2555
Volume : 54, Issue 8, No.1, August : 2025

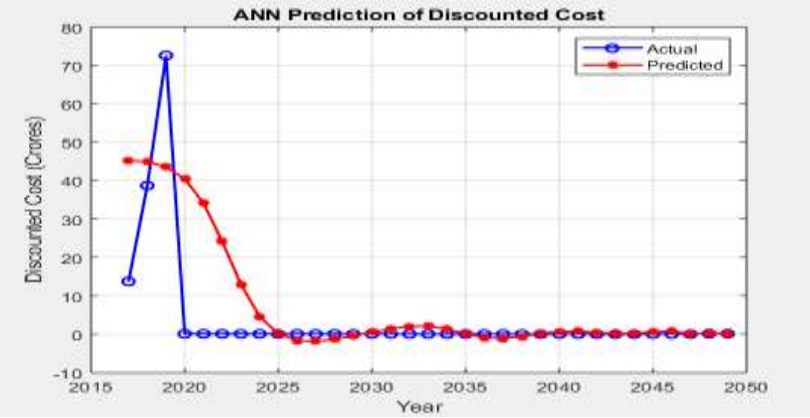

Figure no.4: ANN prediction of Discounted Cost

The graph shows the ANN (Artificial Neural Network) prediction of discounted costs over time, from 2015 to 2050. The y-axis represents the discounted cost in crores, while the x-axis represents the years. The blue line with circles shows the actual discounted cost values, and the red line with stars represents the predicted values by the ANN model.

Initially, the actual cost fluctuates significantly, peaking around 2020 at about 75 crores, then rapidly drops to near zero by 2023. The predicted values start high at around 45 crores in 2015 and gradually decline, aligning with actual values near zero around 2025. From 2025 onwards, both actual and predicted costs remain low, oscillating slightly around zero with predicted values closely matching actual costs, showing the model's accuracy in long-term forecasting. This plot indicates that the ANN model effectively captures the trend and magnitude of discounted costs over time, particularly excelling in the long-term predictions where values stabilize near zero.

4.2 Annual maintenance for Tunnel + Flexible Tunnel

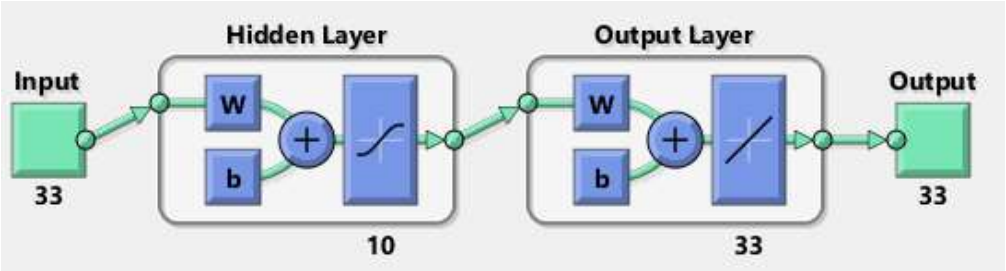

Figure no.5: Hidden and Output Layer

The image depicts a simple neural network architecture with one hidden layer and one output layer. The input layer has 33 nodes, which feed into a hidden layer containing 10 nodes. Each node in the hidden layer has weights (W) and biases (b) applied, followed by an activation function. The output from the hidden layer then passes to the output layer, which consists of 33 nodes, each also with weights, biases, and an activation function, producing a final output of 33 nodes.

This structure is similar to the annual maintenance cost table for Tunnel + Rigid Pavement shown. The table calculates the annual maintenance costs and discounted values over years, reflecting a detailed process like the stepwise transformation in the neural network. Both represent a systematic progression—one through layers of computation (neural network) and the other through years of maintenance costs considering inflation and discounting, ultimately summarizing the net present value over time for the civil construction and maintenance costs.

Industrial Engineering Journal
ISSN: 0970-2555
Volume : 54, Issue 8, No.1, August : 2025

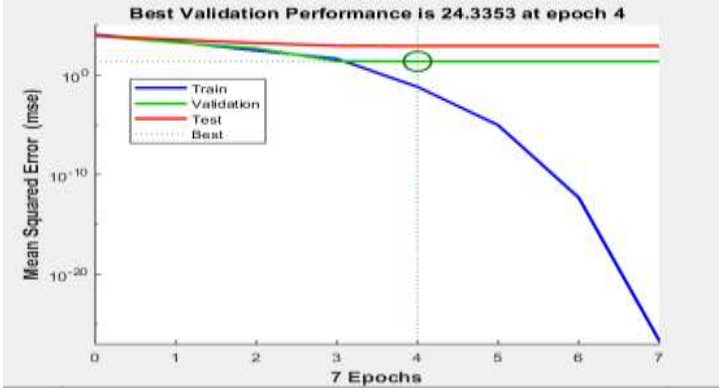

Figure no.6: Best Validation Performance

The graph shows the mean squared error (MSE) trends for training, validation, and test datasets over 7 epochs, with the best validation performance achieved at epoch 4 (MSE ≈ 24.3353). Initially, all three errors start similarly but diverge as epochs progress. The training error (blue line) decreases significantly after epoch 4, indicating the model fits the training data better. However, validation (green) and test (red) errors remain relatively flat and higher, suggesting possible overfitting. The best validation error is marked with dotted lines and a green circle at epoch 4. This early stopping point balances training accuracy and generalization. The logarithmic scale of the y-axis emphasizes the rapid decline in training error compared to validation and test errors. The figure highlights that although training error reduces drastically, validation and test errors plateau, indicating that continuing training beyond epoch 4 may not improve model generalization.

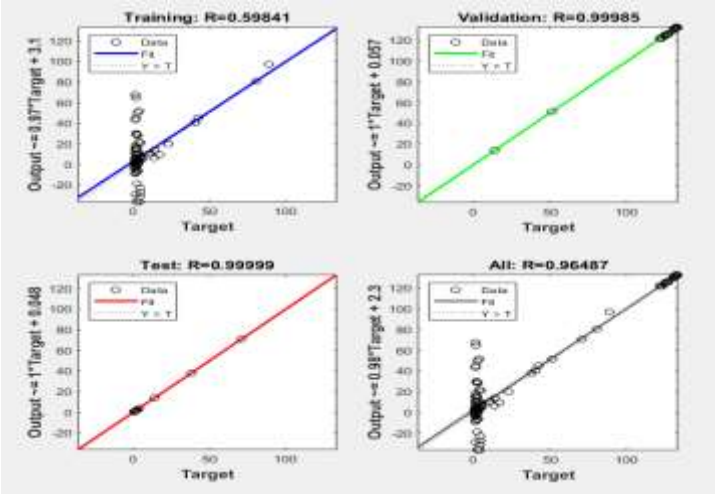

Figure no.7: Best Training, Validation and Test

The table presents a life cycle cost comparison between tunnels with flexible pavement and those with rigid pavement, factoring in a 5% inflation rate and a 12% discount rate. Initially, in 2017, the construction cost of rigid pavement tunnels is higher by 3.06% compared to flexible pavement tunnels, with cumulative costs of 13.77 and 13.36 respectively. Over the years, cumulative costs for both types increase, but flexible pavement remains cheaper until the year 2030, which marks the break-even point where costs nearly equalize at approximately 126.00 for rigid and 126.39 for flexible pavement. After this point, flexible pavement costs surpass those of rigid pavement, rising to 132.35 by 2048 compared to 126.73 for rigid pavement. This indicates that, over a 30-year span, rigid pavement proves more cost-effective, being cheaper by 4.24%, highlighting its long-term economic advantage despite higher initial costs.

Industrial Engineering Journal
ISSN: 0970-2555
Volume : 54, Issue 8, No.1, August : 2025

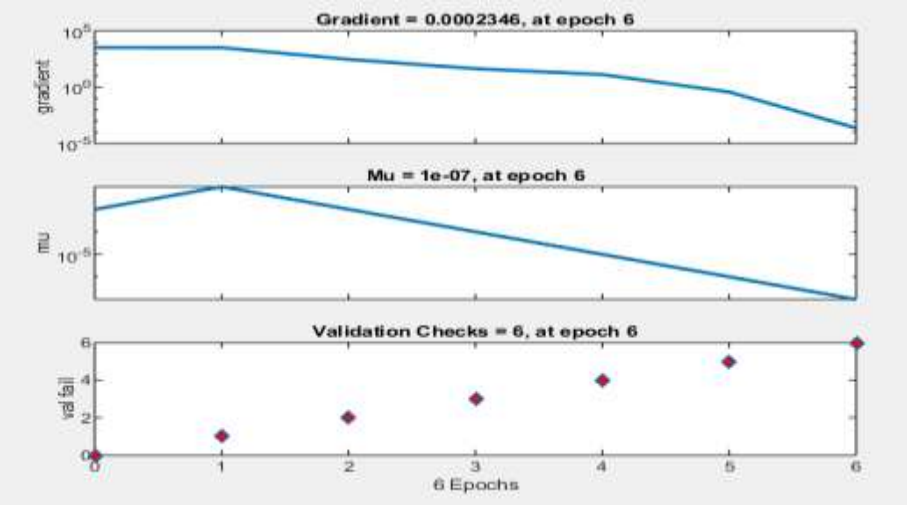

Figure no.8: Gradient and Validation checks

The given image shows the training progress of a machine learning model over six epochs through three plots. The first plot displays the gradient magnitude, which decreases significantly from around 10^5 to near 10^-5, indicating that the model's parameters are stabilizing and the training is converging. The second plot shows the learning rate (mu), which also decreases steadily from roughly 10^-5 to 10^-7, suggesting that the optimization algorithm is reducing step sizes to fine-tune the model carefully. The third plot represents validation checks (val fail), increasing linearly from 0 to 6, implying that the model is failing validation at each epoch, signaling potential overfitting or poor generalization. Overall, the decreasing gradient and learning rate show that the training is progressing, but the continuous validation failures indicate that the model may not be improving in terms of validation accuracy, requiring adjustments in training or model design.

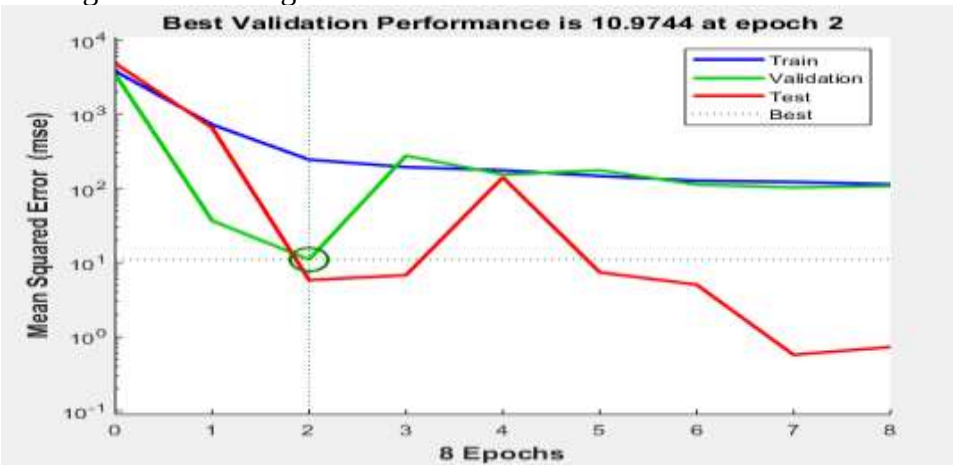

Figure no.9: Best Validation Performance

The plot shows the mean squared error (MSE) performance of a model during training, validation, and testing over 8 epochs. The vertical axis is logarithmic, displaying MSE values ranging from 0.1 to 10,000, while the horizontal axis represents the number of epochs. The blue line (Train) shows a steady decrease in error but stabilizes around 100. The green line (Validation) decreases rapidly initially, reaching the lowest error of approximately 10.97 at epoch 2, highlighted by a vertical dotted line and a circled point. After epoch 2, validation error fluctuates, indicating potential overfitting. The red line (Test) starts high but dramatically drops to below 1 by epoch 7, indicating improved test performance. The legend clarifies

the color coding and the best validation point. The best validation performance at epoch 2 signifies the model's optimal point before overfitting, with MSE around 10.9744, guiding model selection for balancing accuracy and generalization.

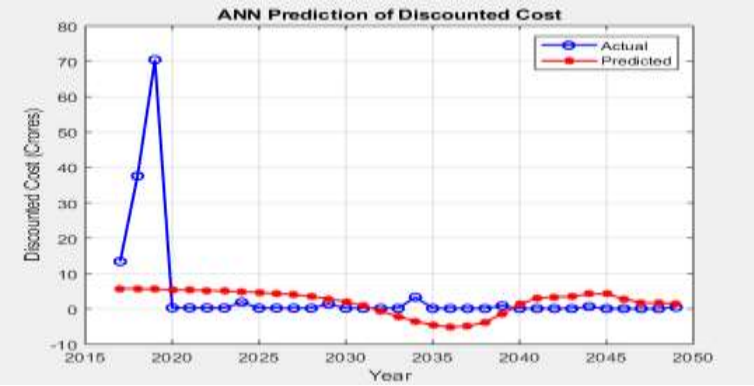

Figure no.10: ANN Prediction of Discounted cost

The graph titled "ANN Prediction of Discounted Cost" compares actual and predicted discounted costs (in crores) over time from 2015 to 2050. The blue line with circles represents the actual costs, while the red line with dots shows the predicted costs by an Artificial Neural Network (ANN). Initially, from 2015 to around 2020, actual costs exhibit sharp fluctuations, peaking near 70 crores, whereas predicted costs remain relatively stable around 5-6 crores. Post-2020, actual costs drop significantly and stabilize close to zero, showing minor fluctuations until 2050. The predicted costs gradually decrease from about 5 crores, dip below zero near 2035, and then slowly rise again, aligning more closely with actual values toward 2050. Overall, the ANN model captures the trend but underestimates early volatility and shows smoother predictions throughout. This comparison highlights the model's strength in trend prediction but also its limitations in capturing sharp real-world fluctuations.

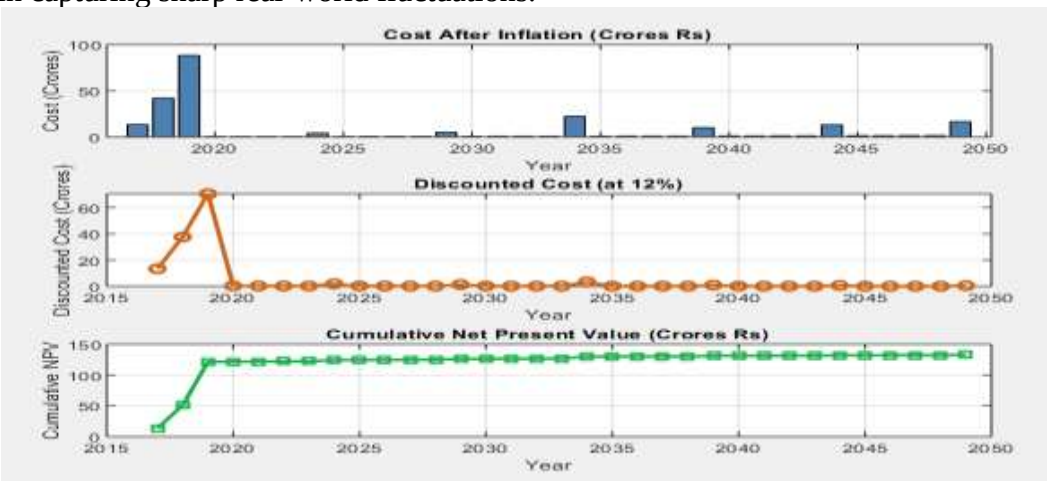

Figure no.11: Cost After Inflation

The image presents three related financial plots over the years from 2015 to 2050, focusing on cost and value adjustments considering inflation and discount rates. The top plot shows the "Cost After Inflation" in crores of rupees, indicating that costs are significantly higher in the initial years (2018-2020), with a peak around 90 crores, followed by much smaller costs spread out sporadically in later years. The middle plot depicts the "Discounted Cost (at 12%)," where initial costs peak sharply around 2018-2020 but quickly diminish, reflecting the present value of future costs discounted at a 12% rate, making later costs

almost negligible in value. The bottom plot illustrates the "Cumulative Net Present Value (NPV)," which starts low but sharply rises around 2018-2020 to approximately 140 crores and then plateaus, indicating that most value is accumulated early, and later costs or benefits have minimal impact on the total NPV. Overall, the charts show early high costs with major financial impact and minimal long-term discounted costs, emphasizing the importance of initial investments in determining net value.

Comparative Analysis

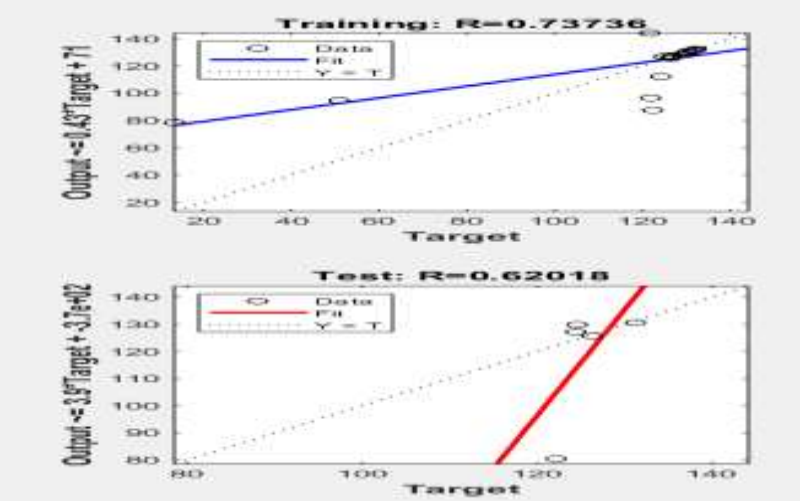

Figure no.12: Training and Test

The image displays two scatter plots illustrating the relationship between predicted outputs and target values for a model during training and testing phases. The top plot, labeled "Training: R=0.73736," shows data points scattered around a blue fitted line representing the model's predictions. The closer the points are to this line, the better the fit. The dotted line represents the ideal scenario where predicted output equals the target (Y = T). The R-value of 0.73736 indicates a moderate positive correlation during training, meaning the model predictions reasonably align with actual targets, though some variability exists. The bottom plot, labeled "Test: R=0.62018," shows test data with points scattered around a red fitted line, but this line diverges more from the ideal dotted line. The R-value of 0.62018 indicates a weaker correlation in the test phase, suggesting the model's predictive power decreases on unseen data. This difference between training and testing performance indicates potential overfitting or limitations in generalization capability.

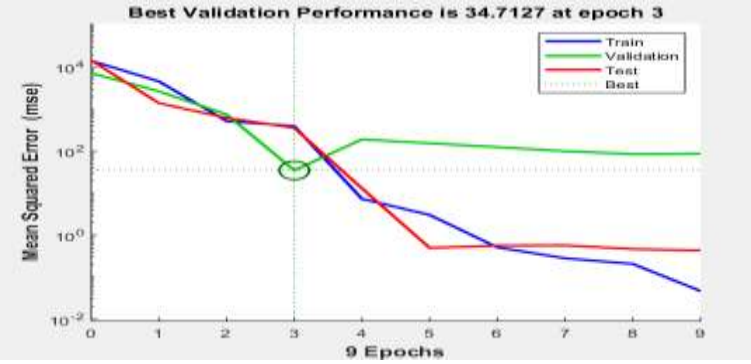

Figure no.13: ANN Performance Matrix

The graph depicts the training, validation, and test mean squared error (MSE) over 9 epochs for a machine learning model. The vertical axis is logarithmic, showing the MSE values, while the horizontal axis

represents the number of epochs. The blue line indicates the training error, which steadily decreases over time, reflecting the model's improving fit to the training data. The red line shows the test error, which follows a similar downward trend. The green line represents validation error, which decreases initially but rises slightly after epoch 3, indicating potential overfitting. The plot highlights the best validation performance of 34.7127 MSE, achieved at epoch 3, marked by vertical and horizontal dotted lines. This epoch is crucial because the validation error is minimized, signifying the optimal balance between underfitting and overfitting. The graph helps in selecting the best epoch for early stopping to ensure generalization on unseen data, avoiding training beyond the point where validation error increases.

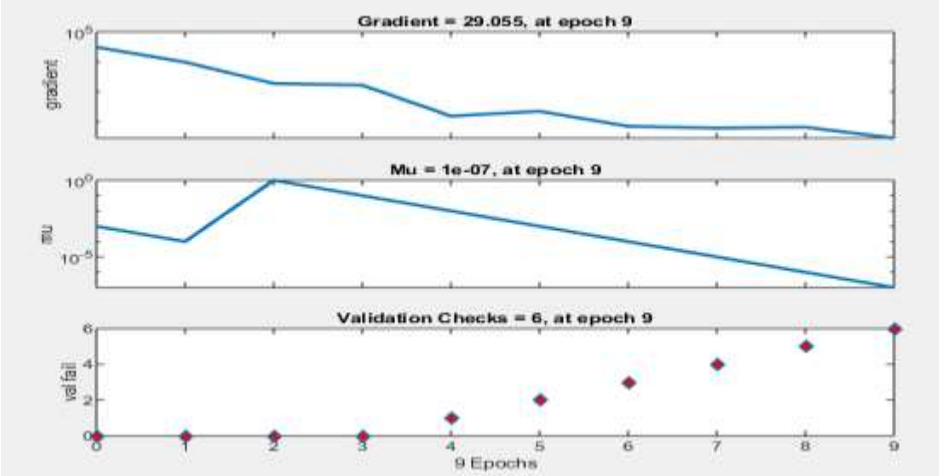

Figure no.14: Training States

The image shows three-line plots depicting the training progress of a machine learning model over 9 epochs. The top plot tracks the gradient, which starts very high (around 10^5) and decreases significantly by epoch 9 to about 29.055, indicating that the model is converging as the updates become smaller. The middle plot displays the learning rate parameter "Mu," which initially increases to 10^-4 but then steadily decreases to 10^-7 by epoch 9, showing an adaptive adjustment to control the step size during training. The bottom plot shows the validation failures ("val fail"), which remain zero for the first three epochs but then start increasing linearly from epoch 4 to 9, reaching 6 at epoch 9. This suggests that the model is encountering more validation errors as training progresses, possibly due to overfitting or increased difficulty in improving validation performance. Overall, the plots indicate decreasing gradients and learning rate with rising validation errors at epoch 9.

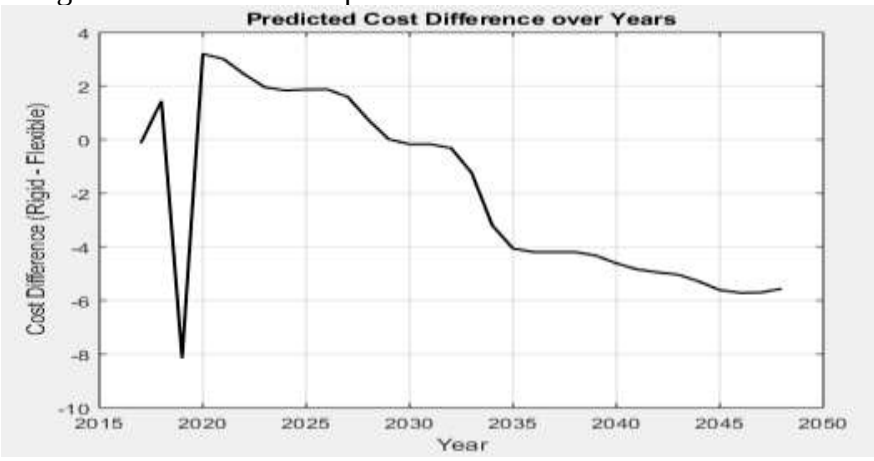

Figure no.14: Predicted Cost Difference over years

Industrial Engineering Journal
ISSN: 0970-2555
Volume : 54, Issue 8, No.1, August : 2025

The graph titled "Predicted Cost Difference over Years" illustrates the projected cost difference between rigid and flexible options from 2015 to 2050. The y-axis represents the cost difference (Rigid - Flexible), while the x-axis shows the years. Initially, around 2015, the cost difference is slightly positive, indicating rigid options are costlier. However, a sharp dip occurs around 2018, showing a significant negative difference of about -8, meaning flexible options were more expensive then. Following this, the cost difference rises dramatically, peaking around 2019-2020 with rigid options costing roughly 3 units more. After 2020, the cost difference steadily declines, crossing zero around 2030 and becoming increasingly negative. By 2050, the cost difference stabilizes near -5.5, implying flexible options become more cost-effective over time. This trend suggests a future economic advantage in using flexible solutions compared to rigid ones, likely due to advancements or cost reductions in flexible technology.

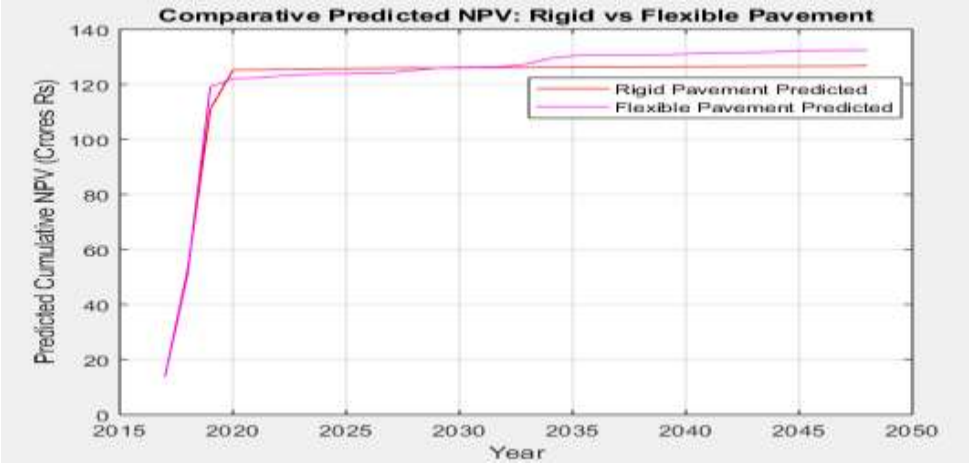

Figure no.15: Comparative Predicted NPV

The graph compares the predicted cumulative Net Present Value (NPV) in crores of rupees for rigid and flexible pavements over a period from 2015 to 2050. Both pavement types show a rapid increase in NPV from 2015 to around 2020, with rigid pavement reaching approximately 125 crores Rs and flexible pavement slightly lower but closely trailing. After 2020, the NPVs for both pavements plateau, indicating a stabilization in predicted returns. However, flexible pavement continues to show a marginal increase beyond 2020, reaching around 135 crores Rs by 2050, whereas rigid pavement remains almost flat just above 125 crores Rs. This suggests that flexible pavement may offer slightly higher long-term economic benefits compared to rigid pavement. Overall, while both types yield significant returns early on, flexible pavement is projected to outperform rigid pavement in the long run in terms of cumulative predicted NPV.

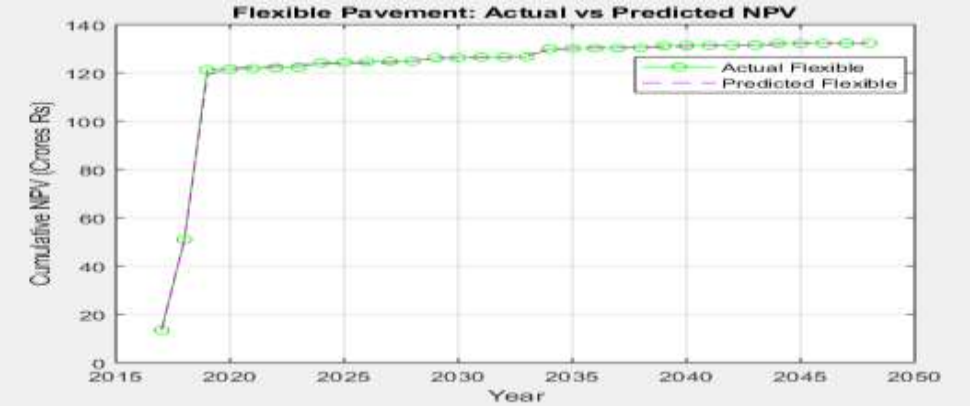

Figure no.16: Flexible Pavement

The graph depicts the cumulative Net Present Value (NPV) for flexible pavement over time, comparing actual versus predicted values from 2015 to 2050. The Y-axis shows the cumulative NPV in crores of rupees, while the X-axis represents the years. Both the actual and predicted NPV values start low around 2015 but rapidly increase until 2020, reaching around 120 crores. After 2020, the NPV values gradually rise and stabilize around 130 crores. The actual flexible pavement NPV is represented by green circles connected with a solid line, while the predicted NPV is shown as a dashed magenta line. The close alignment of the two lines indicates that the predicted NPV closely matches the actual NPV values throughout the period, reflecting a reliable prediction model for flexible pavement investment returns over time.

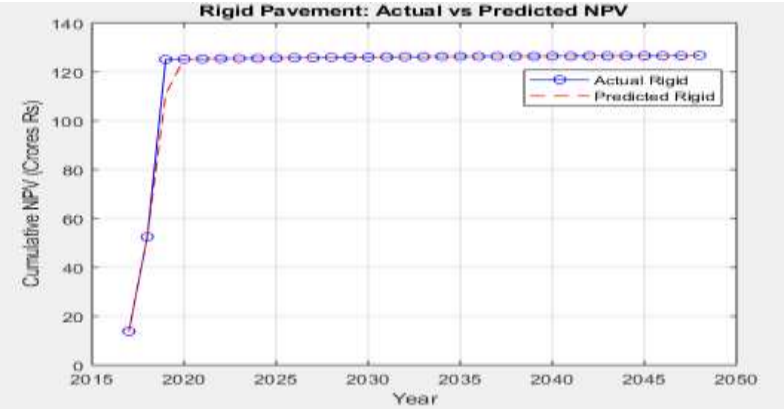

Figure no.16: Rigid Pavment

The graph titled "Rigid Pavement: Actual vs Predicted NPV" compares the cumulative Net Present Value (NPV) of rigid pavement over time, from 2015 to 2050. The vertical axis represents the cumulative NPV in Crores of Rupees, while the horizontal axis marks the years. Two lines are plotted: the blue line with circles shows the actual NPV, and the red dashed line shows the predicted NPV. Both lines begin at a low value in 2015, rise sharply until 2020, reaching approximately 130 Crores Rs, and then plateau, remaining steady until 2050. The close overlap of the actual and predicted lines indicates a strong agreement between the model's prediction and the actual observed data. This suggests that the prediction model for the rigid pavement's NPV is highly accurate in forecasting long-term financial outcomes. The stability in NPV after 2020 indicates no further significant financial changes expected in the pavement's value over the following decades.

5. CONCLUSION

The life cycle cost analysis (LCCA) of the New Austrian Tunneling Method (NATM) using Artificial Neural Networks (ANN) provides a robust framework for evaluating the economic efficiency and sustainability of tunnel construction projects over their entire lifespan. NATM, known for its adaptability to varying geological conditions and its reliance on the surrounding rock for support, presents complex cost implications due to dynamic factors such as excavation methods, support systems, maintenance requirements, and operational conditions. By integrating ANN into LCCA, this study demonstrates an advanced approach to predict and optimize cost parameters, thereby enhancing decision-making in the early design and planning stages. ANN models, trained on historical project data, can identify patterns and correlations that traditional analytical methods might overlook. This enables a more precise estimation of total life cycle costs, incorporating direct construction expenses, indirect costs, future maintenance, and potential risks. The application of ANN not only improves the accuracy of cost forecasting but also supports scenario analysis, allowing stakeholders to evaluate alternative designs and construction

strategies under varied economic and environmental conditions. The research concludes that the combination of NATM and ANN-based LCCA significantly improves the efficiency, reliability, and transparency of cost management in tunnel projects. It empowers engineers and project managers with a predictive tool to mitigate financial risks and optimize resource allocation, ultimately contributing to more cost-effective and sustainable infrastructure development. The study recommends further exploration of hybrid AI models and continuous data collection to enhance predictive capabilities and adapt to evolving construction technologies.

REFERENCES

[1] K. Petroutsatou, A. Maravas, and A. Saramourtsis, "A life cycle model for estimating road tunnel cost," *Tunnelling and Underground Space Technology*, vol. 111, p. 103858, May 2021, doi: 10.1016/j.tust.2021.103858.

[2] F. Davies, L. Moutinho, and B. Curry, "ATM user attitudes: a neural network analysis," *Marketing Intelligence & Planning*, vol. 14, no. 2, pp. 26–32, Apr. 1996, doi: 10.1108/02634509610110778.

[3] A. Qazi, H. Fayaz, A. Wadi, R. G. Raj, N. A. Rahim, and W. A. Khan, "The artificial neural network for solar radiation prediction and designing solar systems: a systematic literature review," *Journal of Cleaner Production*, vol. 104, pp. 1–12, Oct. 2015, doi: 10.1016/j.jclepro.2015.04.041.

[4] M. Rafie and F. Samimi Namin, "Prediction of subsidence risk by FMEA using artificial neural network and fuzzy inference system," *International Journal of Mining Science and Technology*, vol. 25, no. 4, pp. 655–663, Jul. 2015, doi: 10.1016/j.ijmst.2015.05.021.

[5] O. I. Olanrewaju, A. O. Bello, M. A. Semiu, and S. A. Mudashiru, "Critical barriers to effective communication in the construction industry: evidence from Nigeria," *International Journal of Construction Management*, vol. 25, no. 7, pp. 783–801, May 2025, doi: 10.1080/15623599.2024.2362018.

[6] K. Petroutsatou, A. Maravas, and A. Saramourtsis, "A life cycle model for estimating road tunnel cost," *Tunnelling and Underground Space Technology*, vol. 111, p. 103858, May 2021, doi: 10.1016/j.tust.2021.103858.

[7] E. Hromada, "Real Estate Insights on Mortgage Rates, Apartment Prices, and Rentals in Czech Republic," *IJOES*, vol. 13, no. 1, pp. 13–29, May 2024, doi: 10.52950/ES.2024.13.1.002.

[8] K. W. Seo *et al.*, "Comparative genetic characterisation of third-generation cephalosporin-resistant Escherichia coli isolated from integrated and conventional pig farm in Korea," *Journal of Global Antimicrobial Resistance*, vol. 34, pp. 74–82, Sep. 2023, doi: 10.1016/j.jgar.2023.06.010.

[9] N. Mcneil-Ayuk and A. Jrade, "An Integrated Building Information Modeling (BIM) and Circular Economy (CE) Model for the Management of Construction and Deconstruction Waste Based on Construction Methods," *OJCE*, vol. 14, no. 02, pp. 168–195, 2024, doi: 10.4236/ojce.2024.142009.

[10] N. Dutta, K. Palanisamy, P. Shanmugam, U. Subramaniam, and S. Selvam, "Life Cycle Cost Analysis of Pumping System through Machine Learning and Hidden Markov Model," *Processes*, vol. 11, no. 7, p. 2157, Jul. 2023, doi: 10.3390/pr11072157.

[11] I. Samuelsson, J. Spross, and S. Larsson, "Integrating life-cycle environmental impact and costs into geotechnical design," *Proceedings of the Institution of Civil Engineers - Engineering Sustainability*, vol. 177, no. 1, pp. 19–30, Feb. 2024, doi: 10.1680/jensu.23.00012.

[12] R. S. Hamid, A. Abror, S. M. Anwar, and A. Hartati, "The role of social media in the political involvement of millennials," *SJME*, vol. 26, no. 1, pp. 61–79, May 2022, doi: 10.1108/SJME-08-2021-0151.

[13] Ali Asghar Pilehvar, "Spatial-geographical analysis of urbanization in Iran," *Humanit Soc Sci Commun*, vol. 8, no. 1, p. 63, Mar. 2021, doi: 10.1057/s41599-021-00741-w.

[14] A. A. Alqahtani, "Teachers' perceptions of principals' motivating language and public school climates in Kuwait," *Management in Education*, vol. 29, no. 3, pp. 125–131, Jul. 2015, doi: 10.1177/0892020615584104.

[15] I. Hartl, M. Sorger, K. Hartl, B. J. Ralph, and I. Schlögel, "Passive seismic monitoring in conventional tunnelling – An innovative approach for automatic process recognition using support vector machines," *Tunnelling and Underground Space Technology*, vol. 137, p. 105149, Jul. 2023, doi: 10.1016/j.tust.2023.105149.

[16] I. Hartl, M. Sorger, K. Hartl, B. J. Ralph, and I. Schlögel, "Passive seismic monitoring in conventional tunnelling – An innovative approach for automatic process recognition using support vector machines," *Tunnelling and Underground Space Technology*, vol. 137, p. 105149, Jul. 2023, doi: 10.1016/j.tust.2023.105149.

[17] K. T. Peter *et al.*, "Using High-Resolution Mass Spectrometry to Identify Organic Contaminants Linked to Urban Stormwater Mortality Syndrome in Coho Salmon," *Environ. Sci. Technol.*, vol. 52, no. 18, pp. 10317–10327, Sep. 2018, doi: 10.1021/acs.est.8b03287.

[18] J.-H. Lee *et al.*, "Transgenic expression of a ratiometric autophagy probe specifically in neurons enables the interrogation of brain autophagy *in vivo*," *Autophagy*, vol. 15, no. 3, pp. 543–557, Mar. 2019, doi: 10.1080/15548627.2018.1528812.

[19] J. Lai, J. Qiu, Z. Feng, J. Chen, and H. Fan, "Prediction of Soil Deformation in Tunnelling Using Artificial Neural Networks," *Computational Intelligence and Neuroscience*, vol. 2016, pp. 1–16, 2016, doi: 10.1155/2016/6708183.

[20] P. Farmer *et al.*, "Identification of molecular apocrine breast tumours by microarray analysis," *Breast Cancer Res*, vol. 7, no. S2, p. P2.11, bcr1122, Jun. 2005, doi: 10.1186/bcr1122.

[21] A. Shah *et al.*, "A comprehensive study on skin cancer detection using artificial neural network (ANN) and convolutional neural network (CNN)," *Clinical eHealth*, vol. 6, pp. 76–84, Dec. 2023, doi: 10.1016/j.ceh.2023.08.002.

[22] D. Gianazza, "Forecasting workload and airspace configuration with neural networks and tree search methods," *Artificial Intelligence*, vol. 174, no. 7–8, pp. 530–549, May 2010, doi: 10.1016/j.artint.2010.03.001.

[23] N. F. Davis, S. McGrath, M. Quinlan, G. Jack, N. Lawrentschuk, and D. M. Bolton, "Carbon Footprint in Flexible Ureteroscopy: A Comparative Study on the Environmental Impact of Reusable and Single-Use Ureteroscopes," *Journal of Endourology*, vol. 32, no. 3, pp. 214–217, Mar. 2018, doi: 10.1089/end.2018.0001.

[24] F. B. Ribeiro, F. A. C. D. Nascimento, and M. A. V. D. Silva, "Environmental performance analysis of railway infrastructure using life cycle assessment: Selecting pavement projects based on global warming potential impacts," *Journal of Cleaner Production*, vol. 365, p. 132558, Sep. 2022, doi: 10.1016/j.jclepro.2022.132558.

[25] A. Mousavi, M. Ghasemi-Nejad-Raeini, M. Taki, and B. Elhami, "Energy and Environmental Analysis of Different Methods for Using Bagasse from Sugarcane by Life Cycle Assessment Approach," *Sugar Tech*, vol. 27, no. 3, pp. 783–797, Jun. 2025, doi: 10.1007/s12355-025-01536-y.

[26] M. Price, S. Raghunathan, and R. Curran, "An integrated systems engineering approach to aircraft design," *Progress in Aerospace Sciences*, vol. 42, no. 4, pp. 331–376, Jun. 2006, doi: 10.1016/j.paerosci.2006.11.002.

[27] D. L. Van Schalkwyk, M. Mandegari, S. Farzad, and J. F. Görgens, "Techno-economic and environmental analysis of bio-oil production from forest residues via non-catalytic and catalytic pyrolysis processes," *Energy Conversion and Management*, vol. 213, p. 112815, Jun. 2020, doi: 10.1016/j.enconman.2020.112815.

[28] E. S. Yu and C. Y. R. Chen, "Traffic prediction using neural networks," in *Proceedings of GLOBECOM '93. IEEE Global Telecommunications Conference*, Houston, TX, USA: IEEE, 1993, pp. 991–995. doi: 10.1109/GLOCOM.1993.318226.

[29] C. Y. Kim, G. J. Bae, S. W. Hong, C. H. Park, H. K. Moon, and H. S. Shin, "Neural network based prediction of ground surface settlements due to tunnelling," *Computers and Geotechnics*, vol. 28, no. 6–7, pp. 517–547, Sep. 2001, doi: 10.1016/S0266-352X(01)00011-8.

[30] Y. Zhang, J. Joiner, S. H. Alemohammad, S. Zhou, and P. Gentine, "A global spatially contiguous solar-induced fluorescence (CSIF) dataset using neural networks," *Biogeosciences*, vol. 15, no. 19, pp. 5779–5800, Oct. 2018, doi: 10.5194/bg-15-5779-2018.